Universal thermopower of bad metals

V. Zlatić,[1,2] G. R. Boyd,[2] and J. K. Freericks[2]

[1]*Institute of Physics, Zagreb POB 304, Croatia*

[2]*Department of Physics, Georgetown University, Washington, DC 20057, USA*

"Bad metals" are known to have a large linear resistivity at high T that is universally seen near the Mott-Hubbard insulating phase. Less well known is that the thermopower $\alpha(T)$ of the Mott-Hubbard systems also exhibits simple universal features: (i) close to the insulating phase, where the resistivity has a low-temperature upturn, $\alpha(T)$ has a pronounced low-T peak that shifts to higher T with doping; (ii) when the resistivity is nearly linear, which occurs at moderate doping, $\alpha(T)$ has a small low-T peak that shifts to lower T with doping and has a high-T sign change; and (iii) at the highest doping, where the resistivity acquires a T^2 term, $\alpha(T)$ is negative and depends monotonically on T. The universality $\alpha(T)$ can be understood using the Kelvin formula and the fact that the chemical potential for doped Mott insulators displays similar behavior at high T. The universality is illustrated with the exact solution of the simplest model for a doped Mott insulator at high T.

I. INTRODUCTION

Among the defining features of bad metals is a large but metallic resistivity and a thermopower which grows to much larger values than in normal metals. Their resistivity is often (quasi)linear at high temperatures, continuing to increase as a function of temperature beyond the minimal metallic conductivity of the Mott-Ioffe-Regel limit [1,2]. Since the mean free path inferred from the Drude formula drops below one lattice spacing, it is difficult to describe charge and heat transport in terms of quasiparticle currents, and the Fermi-liquid paradigm fails.

Less well known is that, depending on the concentration of carriers, the thermopower $\alpha(T)$ of Mott-Hubbard systems exhibits (quasi)universal features. This can be used to classify a wide range of different strongly correlated materials into well-defined groups: (i) at very low carrier concentration (lightly doped Mott insulators with a low-T upturn in the resistivity), $\alpha(T)$ has a pronounced low-T peak that shifts to higher T with doping; (ii) at moderate carrier concentration (bad metals with a resistivity that is nearly linear in temperature), $\alpha(T)$ has a small low-T peak that shifts to lower T with doping and has a high-T sign change; and (iii) at the highest carrier concentration (dirty Fermi liquids with a well-defined T^2 term in the resistivity), $\alpha(T)$ is negative and depends monotonically on T.

The variation of the thermopower with the carrier concentration has been studied most thoroughly in vanadates $La_{1-x}Sr_xVO_3$ [3], cobaltates [4], and cuprates [5–7]. Those experiments show that doping first transforms a Mott-Hubbard insulator into an "underdoped" bad metal and then into an "overdoped" dirty Fermi liquid. In other materials, like iron silicide FeSi [8], iron antimodide $FeSb_2$ [9,10], sodium doped cobalt oxide Na_xCoO_2 [11], misfit cobaltites [12], and several other oxides [13], the carrier concentration is more difficult to change and the thermopower of each particular system exhibits only one of the above described features. Nevertheless, it is difficult to imagine that such universal behavior, seen in so many compounds, does not have a simple underlying explanation. We provide such an explanation in this work.

Considering the enormous difference in the structural and electronic properties of the strongly correlated materials used in the above studies, the universal behavior of the thermopower suggests that the transport properties of the high-temperature phase are the consequence of a large on-site Coulomb interaction and might be described by an effective band of strongly correlated electrons. (The approach we take here is similar to the spin-1/2 Anderson model describing the Kondo effect in real materials.) Indeed, the explanation involves three simple observations: (i) at high temperature, above the renormalized Fermi-liquid temperature, the density of states (DOS) of correlated materials is dominated by upper and lower Hubbard bands; (ii) the chemical potential, which is determined primarily by the overall shape of the DOS, has a similar T dependence at high temperature; and (iii) the thermopower is well approximated by the Kelvin formula, which relates it to the temperature derivative of the chemical potential. These features are not universal in the thermodynamic sense of a scaling function, and the Kelvin formula is not always quantitatively accurate, but for dozens of materials the temperature dependence of the chemical potential, for a system with an upper and lower "Hubbard" band in the DOS, will always follow a similar pattern. It is in this limited sense that the behavior of the thermopower is "universal."

For large correlation, regardless of the details of a particular microscopic description, the DOS has a Mott-Hubbard gap, the optical conductivity is characterized by the transfer of spectral weight from the low-energy Drude peak to the high-energy incoherent background, the resistivity is linear, and the thermopower has anomalous behavior. This is precisely what is seen in the Hubbard model at high temperature, and it is the universal features of this bad metal phase that we describe here. Several recent papers used a single band model to discuss the effects of strong correlation on the transport properties of bad metals [14–16]. Because the properties of the thermopower are universal in the sense described above, we need only find a model that describes a doped Mott insulator above its Fermi-liquid temperature. Here, we use the spinless Falicov-Kimball model [17], which is closely related to the Hubbard model

[18] but has the advantage that it admits an exact numerically tractable solution at any doping. However, one should not use it to infer microscopic properties for materials discussed above.

In Sec. II, we define the model and describe its solution. In Sec. III, we present our results, and we conclude in Sec. IV.

II. MODEL AND CALCULATIONS

The model is defined by the Hamiltonian

$$H = -\frac{t^*}{\sqrt{Z}} \sum_{ij} c_i^\dagger c_j + U \sum_i w_i c_i^\dagger c_i - (\Delta\mu + \mu_0) \sum_i c_i^\dagger c_i,$$ (1)

where the summation is over N lattice sites, $c_i^\dagger$ (c_i) is the itinerant electron creation (annihilation) operator, and $w_i = f_i^\dagger f_i$ is one or zero and represents the number operator of a localized electron on site i. U is the interaction strength and t^* is the hopping scaled so that we can properly take the infinite coordination number ($Z \to \infty$) limit (the hopping is between nearest neighbors only). We work on a Bethe lattice, measure the energy with respect to the zero-temperature chemical potential μ_0 ($\mu = \Delta\mu + \mu_0$), and rescale the Hamiltonian by t^*, which makes the Green's functions and the self-energy dimensionless. Localized electrons are distributed according to an annealed thermodynamic ensemble, and $\sum_i w_i/N = w_1$ is their average filling. There are N_c itinerant electrons per site and we take $N_c = w_1$ to describe the so-called simplified Hubbard model in a paramagnetic phase. We dope away from half filling, so $w_1 = 0.5 - \delta = N_c$, where δ is the doping (or density of itinerant holes n_h). Note that the total number of holes is 2δ and that the critical doping densities for defining the different regimes will vary with the explicit models chosen. At high enough temperatures, the results obtained for $w_1 = N_c$ provide a good approximation to the Hubbard model (by taking the up-spin electrons as the mobile electrons and the down-spin electrons as the localized ones). The two models differ at low T where coherence sets into the Hubbard model, creating Fermi-liquid phases or different forms of ordered phases, but that is irrelevant for the universal properties of the thermopower that we describe here.

The solution is obtained by employing dynamical mean-field theory (DMFT) [19–21]. We focus on the local retarded Green's function $G_{loc}(\omega)$, defined in Ref. [21], and utilize the conventional DMFT algorithm to formulate the solution. On the Bethe lattice, $G_{loc}(\omega)$ satisfies a cubic equation [18] that we solve numerically, and the self-energy is then given by the expression

$$\Sigma(\omega) = \omega + \mu - G_{loc}(\omega) - \frac{1}{G_{loc}(\omega)},$$ (2)

where we set $t^* = 1$.

The electrical conductivity σ, the thermopower α, and the thermal conductivity κ_e are calculated by linear response theory [22]. This gives $\sigma(T) = \sigma_0 L_{11}(T)$, $\alpha(T) = (k_B/e)L_{12}/(T L_{11})$, and $\kappa_e = (k_B/e)^2(\sigma/T)(L_{22}/L_{11} - L_{12}^2/L_{11}^2)$, where $\sigma_0 = e^2/(\hbar Z a)$ with a an effective lattice spacing,

$$L_{mn}(T) = \int_{-\infty}^{\infty} d\omega \left(-\frac{\partial f(\omega)}{\partial \omega} \right) \omega^{m+n-2} \Lambda_{tr}(\omega)$$ (3)

is the transport integral, and $f(\omega) = 1/(1 + e^{\omega/T})$ is the Fermi function. The transport function is

$$\Lambda_{tr}(\omega) = \frac{4}{3\pi^2} \int d\epsilon \, \Phi(\epsilon)[\text{Im}G(\epsilon,\omega)]^2,$$ (4)

where ϵ is the noninteracting band energy, $\Phi(\epsilon)$ is the noninteracting transport DOS (DOS weighted by the square of the velocity), and $G(\epsilon,\omega)$ is the dimensionless Green's function of conduction electrons calculated within DMFT. Using $\Phi(\epsilon) = (4 - \epsilon^2)\sqrt{4 - \epsilon^2}/2\pi$, the transport function can be calculated exactly, with the result [23]

$$\Lambda_{tr}(\omega) = \frac{1}{3\pi^2} \text{Im}^2[G_{loc}(\omega)]\left(\frac{|G_{loc}(\omega)|^2 - 3}{|G_{loc}(\omega)|^2 - 1} \right).$$ (5)

The numerical data show that the thermopower is well approximated by the "thermodynamic" Kelvin formula [24], $\alpha_K(T) = -(k_B/q_e)(\partial\mu/\partial T)$, which is obtained by assuming that the diffusion of δn particles of charge q_e, driven by the thermal force $\Delta T/T$, changes the entropy by δs and
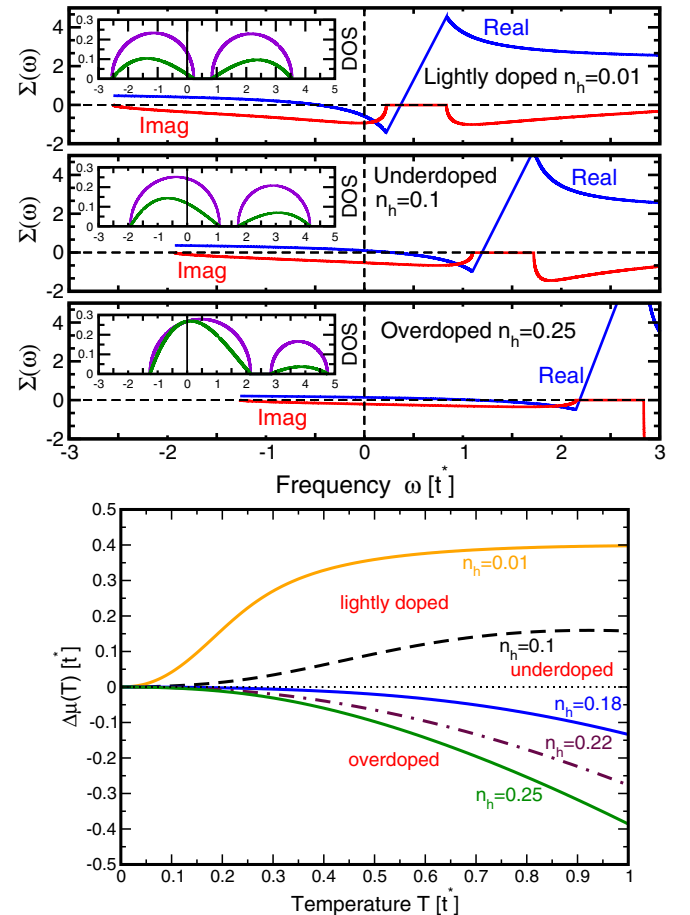

FIG. 1. (Color online) Upper panels: The real part (blue, above) and the imaginary part (red, below) of the self-energy are plotted vs energy for $U = 3$ and for various dopings. The energy is measured with respect to the zero-temperature chemical potential μ_0, in units of t^*. Inset: The local DOS (violet, above) and the transport DOS (green, below) at $T = 0$. Lower panel: The chemical potential $\Delta\mu(T)$, measured with respect to μ_0, for various dopings.

the voltage by ΔV. In a stationary state without any charge current, the loss of the thermal energy due to the heat flow, $\delta s \times \Delta T$, is balanced by the work done against the electrical field, $q_e \delta n \times \Delta V$. Thus, $\Delta V / \Delta T = (1/q_e)(\delta s / \delta n)$ and the Kelvin formula follows from the appropriate Maxwell relation. Unlike the Kubo formula, which is obtained by making the driving fields uniform before they become static, the Kelvin formula is derived by taking the static limit first; the fact that it works for strongly correlated systems is somewhat surprising. As pointed out by Arsenault *et al.* [16], a good agreement between $\alpha_K(T)$ and $\alpha(T)$ can be taken as an indication that transport properties are mainly determined by the equilibrium fluctuations, i.e., by the renormalized DOS. At very high temperatures, the Kelvin formula reduces to the Heikes formula, $\alpha_H(T) = -(k_B/e)(\mu/T)$, which is often used in the experimental literature to discuss the concentration dependence of the thermopower of oxides [13]. The difficulty with $\alpha_H(T)$ is that it only holds in the atomic limit, when the entropy and thermopower are constant. The Kelvin formula, on the other hand, is equally simple but provides an expression that can be used to discuss the thermopower in the full temperature range.

III. RESULTS

The numerical calculations are performed for $U = 3$, which produces a Mott-Hubbard insulator at half filling. In the upper panel of Fig. 1, we show the frequency dependence of the zero-temperature self-energy, the local DOS, $\rho_{\rm loc}(\omega) = -{\rm Im} G_{\rm loc}(\omega)/\pi$, and the transport function $\Lambda_{\rm tr}(\omega)$, for various concentrations of holes. At very low doping, the slope of ${\rm Re}\Sigma(\omega)$ and the magnitude of ${\rm Im}\Sigma(\omega)$ at $\omega = 0$ (i.e., at the chemical potential) are very large, making the quasiparticles ill defined. As δ increases, ${\rm Re}\Sigma(0)$ decreases, while ${\rm Im}\Sigma(0)$ increases rapidly up to a maximum. For $\delta > \delta_s$, both ${\rm Re}\Sigma(0)$ and ${\rm Im}\Sigma(0)$ decrease with δ and the low-energy part of ${\rm Im}\Sigma(\omega)$ becomes a linear function of ω. For large δ, ${\rm Im}\Sigma(0)$ becomes very small and an approximate description in terms of (dirty) quasiparticles becomes possible [25].

The temperature dependence of the chemical potential, obtained from the condition $N_c = \int d\omega f(\omega)\rho(\omega) = 0.5 - \delta\rho_{\rm loc}$, where the chemical potential shifts the zero of the function $\rho_{\rm loc}(\omega)$ as temperature changes, is shown in the lower panel of Fig. 1. For small doping, the low-temperature values of $\mu(T)$ are just below the band edge of the lower Hubbard band. An increase of temperature shifts $\mu(T)$ across the band edge,
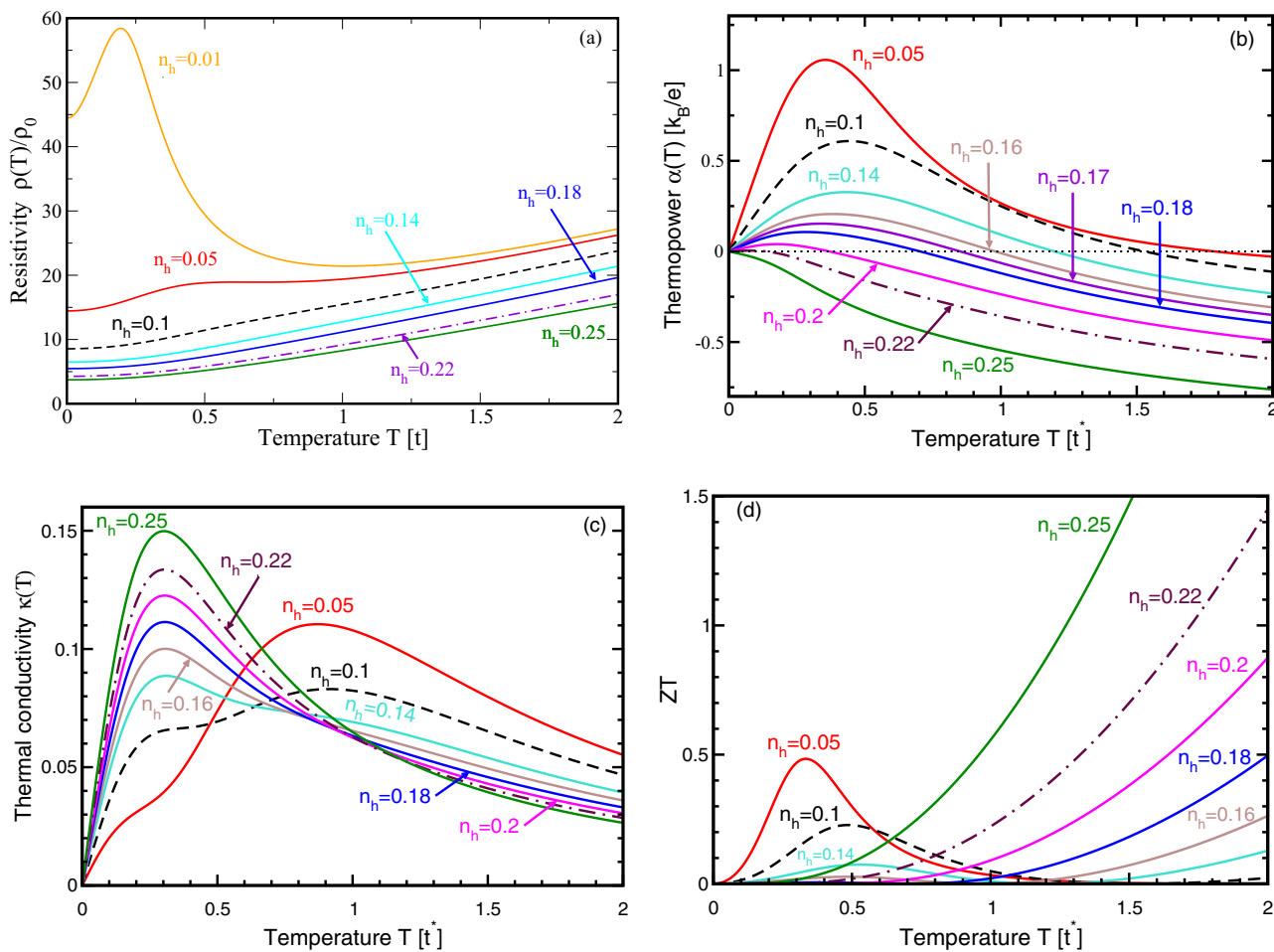

FIG. 2. (Color online) (a) The resistivity $\rho(t)$, (b) thermopower $\alpha(T)$, (c) thermal conductivity $\kappa(T)$, and (d) figure-of-merit ZT plotted vs temperature for $U = 3$ and for various dopings, as indicated in the panels. The boundary between lightly doped insulators and bad metals is indicated by the dashed line; the boundary between the underdoped and overdoped regions is indicated by the dot-dashed line.

toward the center of the gap, which is typical of a doped Mott insulator [15]. At higher doping, μ_0 is closer to the center of the Hubbard band and $\mu(T)$ grows slowly toward a maximum. However, for large enough doping, $\delta > \delta_s(U)$, $\mu(T)$ never crosses the band edge and the model describes an underdoped bad metal ($\delta_s \simeq 0.1$ for $U = 3$). A further increase of doping reduces the initial slope and the high-temperature maximum of $\mu(T)$, until they both vanish at the critical doping, $\delta = \delta_c$, which separates the underdoped and the overdoped regimes ($\delta_c \simeq 0.22$ for $U = 3$). At δ_c, $\mu(T)$ is nearly constant over an extended temperature range and the entropy, considered as a function of doping, assumes a local maximum; the maximum of $\Lambda_{\rm tr}(\omega)$ is now close to $\omega = 0$ and the thermopower is negligibly small. In the overdoped regime, $\delta > \delta_c$, there is a further shift of μ_0 away from the center of the lower Hubbard band and $\mu(T)$ decreases monotonically, as in a Fermi liquid with the same density of holes.

The local DOS and the transport function are shown in the insets of the upper panel of Fig. 1. Doping increases the weight of the lower Hubbard band with respect to the upper one and shifts the maximum of $\rho_{\rm loc}(\omega)$ away from the maximum of $\Lambda_{\rm tr}(\omega)$. For constant impurity concentration, the local DOS and the transport function of the simplified Hubbard model are temperature independent, except for a shift given by $\mu(T)$.

The temperature dependence of the resistivity $\rho(T) = 1/\sigma(T)$, thermopower $\alpha(T)$, thermal conductivity $\kappa_e(T)$, and the electronic figure of merit ZT at various dopings is shown in Fig. 2. The transport functions exhibit three different behaviors, depending on the level of doping. For $\delta \leqslant \delta_s(U)$, the low-temperature transport is not affected by the gap, but at intermediate temperatures, when $\mu(T)$ crosses the band edge, the asymmetry of the electron and hole states is much enhanced. This gives rise to large maxima of $\rho(T)$ and $\alpha(T)$, the breakdown of the Wiedemann-Franz law, and a large ZT. The signatures of lightly doped insulators are the pronounced peaks in $\rho(T)$ and $\alpha(T)$ and the shifts of these peaks to higher temperatures for higher doping [15].

In the underdoped bad metal region, $\delta \gtrsim \delta_s(U)$, transport is completely determined by the incoherent excitations in the lower Hubbard band. The peak in $\rho(T)$ is suppressed and the linear resistivity extends to low temperatures. The thermopower has a low-temperature peak but its height decreases rapidly with δ. Unlike in the lightly doped Mott insulators, the peak of $\alpha(T)$ in (underdoped) bad metals shifts with δ to lower temperatures and, at high temperatures, $\alpha(T)$ changes sign. The low-temperature peak of ZT is rapidly suppressed with doping but at higher temperatures ZT becomes large.

In the overdoped dirty metal region, $\delta \gtrsim \delta_c$, the resistivity is further reduced but the onset of the linear region is pushed to higher temperatures. Below the linear region, $\rho(T)$ exhibits *constant plus* T^2 behavior. The initial slope of $\alpha(T)$ is now negative and $\alpha(T)$, like $\rho(T)$, is a monotonic function of temperature. ZT is very small at low temperature but it grows to large values at high temperatures. Here, Im Σ is sufficiently small that the transport properties can be described in terms of "resilient quasiparticles" [25] or by a dirty Fermi liquid.

The comparison between the thermopowers calculated by the Kelvin and Kubo formulas is shown in Fig. 3. The semiquantitative agreement between $\alpha(T) \simeq \alpha_K(T)$ indicates that the thermodynamic fluctuations are the main cause of
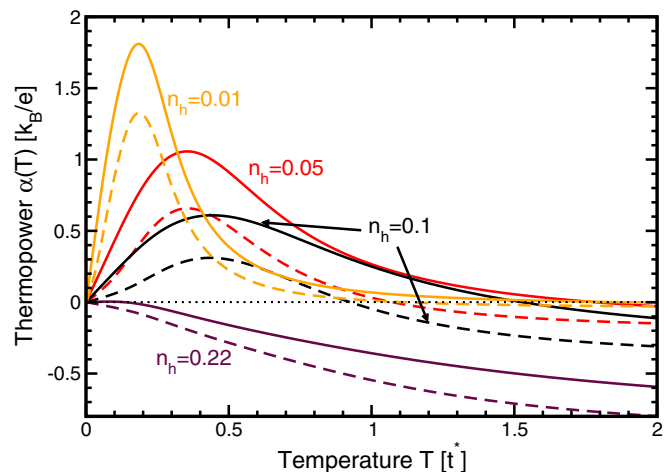

FIG. 3. (Color online) Thermopower obtained from the Kubo formula (full line) compared with the Kelvin formula (dashed line) for various dopings.

transport anomalies. This is at the heart of the universal features seen in the thermopower and the central result of our paper: the chemical potential is a function of the DOS, and the DOS of doped Mott insulators at high temperature share a similar structure for a wide range of different models and materials, so the thermopower will also follow a universal pattern. We have verified that this result also holds in recent calculations of the thermopower for the Hubbard model [26,27].

IV. SUMMARY

We studied the transport properties of bad metals at various dopings using the DMFT solution of the simplified Hubbard model. Since the self-energy functional of this model is known exactly, we found the transport properties at arbitrary doping and obtained the difference between overdoped bad metals and underdoped bad metals. We also studied a slightly doped Mott-Hubbard insulator, which is currently not numerically possible for the systems described by the Hubbard or the Anderson
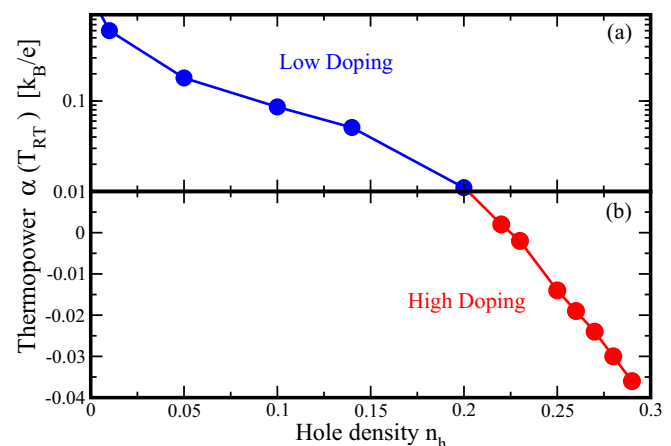

FIG. 4. (Color online) Room-temperature thermopower plotted as a function of the density of itinerant holes. The vertical scale in the upper panel (a) is exponential, while in the lower panel (b) it is linear.

model. In general, we find a linear resistivity and anomalous properties of the thermopower, as observed in the many bad metals mentioned in the introduction.

We find that the simplified Hubbard model qualitatively describes the temperature and doping dependence of the thermopower of many materials with strongly correlated electrons. Taking $T = 0.05$ as room temperature T_{RT} (assuming the hopping satisfies $t^* = 0.5$ eV), we obtain the following features, shown in Fig. 4: (i) the values of $\alpha(T)$ at T_{RT} increase exponentially, when δ is reduced below $\delta_c = 0.2$; (ii) $\alpha(T_{RT})$ changes sign at δ_c; and (iii) for $\delta > \delta_c$, $\alpha(T_{RT})$ is a linear function of δ. These features are seen in the experiments on the cuprates [5–7] but they are yet to be confirmed in other strongly correlated materials mentioned in the introduction.

The universal nature of the thermopower stems from $\mu(T)$, since the Kelvin formula $\alpha_K(T) = -(k_B/q_e)(\partial \mu/\partial T)$ qualitatively captures the exact result. For different doped Mott insulators the chemical potential is a function of the DOS which shares a similar structure for a wide range of different models, once temperature is raised above the coherence temperature.

[1] A. F. Ioffe and A. R. Regel, *Progress in Semiconductors*, edited by A. F. Gibson, Vol. 4 (John Wiley and Sons, New York, 1960), p. 237.

[2] N. E. Hussey, K. Takenaka, and H. Takagi, Philos. Mag. **84**, 2847 (2004).

[3] M. Uchida, K. Oishi, M. Matsuo, W. Koshibae, Y. Onose, M. Mori, J. Fujioka, S. Miyasaka, S. Maekawa, and Y. Tokura, Phys. Rev. B **83**, 165127 (2011).

[4] K. Berggold, M. Kriener, C. Zobel, A. Reichl, M. Reuther, R. Müller, A. Freimuth, and T. Lorenz, Phys. Rev. B **72**, 155116 (2005).

[5] S. D. Obertelli, J. R. Cooper, and J. L. Tallon, Phys. Rev. B **46**, 14928 (1992).

[6] T. Honma and P. H. Hor, Phys. Rev. B **77**, 184520 (2008).

[7] T. M. Benseman, J. R. Cooper, C. L. Zentile, L. Lemberger, and G. Balakrishnan, Phys. Rev. B **84**, 144503 (2011).

[8] B. C. Sales, O. Delaire, M. A. McGuire, and A. F. May, Phys. Rev. B **83**, 125209 (2011).

[9] P. Sun, N. Oeschler, S. Johnsen, B. B. Iversen, and F. Steglich, Phys. Rev. B **79**, 153308 (2009).

[10] Q. Jie, R. Hu, E. Bozin, A. Llobet, I. Zaliznyak, C. Petrovic, and Q. Li, Phys. Rev. B **86**, 115121 (2012).

[11] N. Kaurav, K. K. Wu, Y. K. Kuo, G. J. Shu, and F. C. Chou, Phys. Rev. B **79**, 075105 (2009).

[12] M. Hervieu, A. Maignan, C. Michel, V. Hardy, N. Créon, and B. Raveau, Phys. Rev. B **67**, 045112 (2003).

[13] S. Hebert and A. Maignan, in *Functional Oxides* (Wiley, New York, 2010), Chap. 4.

[14] J. Merino and R. H. McKenzie, Phys. Rev. B **61**, 7996 (2000).

[15] V. Zlatić and J. K. Freericks, Phys. Rev. Lett. **109**, 266601 (2012).

[16] L.-F. Arsenault, B. S. Shastry, P. Sémon, and A.-M. S. Tremblay, Phys. Rev. B **87**, 035126 (2013).

[17] L. M. Falicov and J. C. Kimball, Phys. Rev. Lett. **22**, 997 (1969).

[18] P. van Dongen and C. Leinung, Ann. Phys. (Leipzig) **509**, 45 (1997).

[19] D. Vollhardt, Physica B: Condens. Matter **169**, 277 (1991).

[20] A. Georges, G. Kotliar, W. Krauth, and M. J. Rozenberg, Rev. Mod. Phys. **68**, 13 (1996).

[21] J. K. Freericks and V. Zlatic, Rev. Mod. Phys. **75**, 1333 (2003).

[22] M. Jonson and G. D. Mahan, Phys. Rev. B **21**, 4223 (1980).

[23] A. V. Joura, D. O. Demchenko, and J. K. Freericks, Phys. Rev. B **69**, 165105 (2004).

[24] G. Art and B. S. Shastry, New J. Phys. **13**, 083032 (2011).

[25] X. Deng, J. Mravlje, R. Žitko, M. Ferrero, G. Kotliar, and A. Georges, Phys. Rev. Lett. **110**, 086401 (2013).

[26] M. Kargarian and G. A. Fiete, Phys. Rev. B **88**, 205141 (2013).

[27] G. A. Fiete (private communication).